Ninth International Conference on CFD in the Minerals and Process Industries
CSIRO, Melbourne, Australia
10-12 December 2012

A CFD MODELLING STUDY OF MULTI-PHASE FLOW BEHAVIOUR OF BIOMASS AND BIOCHAR PARTICLES IN A BUBBLING FLUIDIZED BED

Abhishek SHARMA[1], Vishnu PAREEK[1*], Ranjeet UTIKAR[1], Shaobin WANG[1], Hong YANG[2] and Dongke ZHANG[2]

[1] Department of Chemical Engineering, Curtin University, Kent Street, Bentley, Perth, WA 6102, AUSTRALIA
[2] Centre for Energy (M473), The University of Western Australia, 35 Stirling Highway ,Crawley, WA 6009, AUSTRALIA
*Corresponding author, E-mail address: v.pareek@curtin.edu.au

ABSTRACT

Biomass is a promising renewable energy source worldwide. Several modelling and experimental studies have been conducted for biomass thermo-chemical degradation processes, of which, pyrolysis is a significant one due to formation of a variety of products at lower temperature conditions. However, there has not been sufficient information about the hydrodynamics of this process. It is essential to examine the segregation and mixing of different phases in a reactor during biomass pyrolysis. In this work, a multi-phase CFD model for the poly-disperse behavior of biomass in the presence of biochar as bed material in a bubbling fluidized bed has been developed. According to results, the biomass particles behaved as flotsam, while biochar particles behaved as jetsam in the bed. The sensitivity analysis of the effects of operating parameters such as the superficial gas velocity, biomass particle density and diameter on the fluidization behaviour was also conducted.

KEYWORDS: Biomass; Thermo-chemical; Hydrodynamics; Multi-Phase; Mixing/Segregation

NOMENCLATURE

p pressure
v velocity
α volume fraction
ρ density

Subscript
q gas/solid phase
g gas phase
s solid phase

INTRODUCTION

Biomass is considered of great importance for utilization as a potential bio-energy source worldwide. Biomass-derived fuels are currently estimated to contribute around 13% of the world's energy supply (Demirbas et al., 2009). Pyrolysis of biomass is one of the thermo-chemical decomposition processes in which biomass is converted into a carbon-rich solid and volatile matter by heating in the absence of oxygen (Demirbas and Arin, 2002). The solid content of the pyrolysis products is known as the biochar which is generally rich in carbon content. The volatile products of pyrolysis are condensed to give a liquid fraction called the tar or bio-oil (high molecular weight compounds) and a mixture of the non-condensable gases (mainly H_2, CO, CO_2 and C_1-C_4)..

For biomass pyrolysis, the behavior of the biomass particles in the reactor has to be analyzed. Since the biomass particles cannot be uniformly mixed in a reactor system due to their peculiar shapes, sizes and densities, a fluidizing medium such as silica sand is utilized for enhancing mixing and improving heat and mass transfer during the pyrolysis process. There have been few reports which have considered the mixing/segregation behavior of biomass particles with the bed medium in a fluidized bed reactor. Some experimental studies (Rao and Bheemarasetti, 2001; Abdullah et al., 2003; Clarke et al., 2005; Zhong et al., 2008) have been performed only for analyzing the fluidization characteristics of biomass such as minimum fluidization velocities for different mixtures in the reactor. A review of experimental analysis of biomass hydrodynamics in a fluidized bed reactor has been given by Cui and Grace (2007). Zhang et al. (2009) experimentally examined the mixing/segregation pattern by varying mass ratio of biomass (cotton stalk) to sand and superficial gas velocity in the bed. Qiaoqun et al.(2005) carried out experimental as well as modelling study of a mixture of biomass (rice husk) and sand particles for analysing mixing/segregation behavior.

However, modelling and experimental studies so far are not sufficient for evaluating optimal conditions for uniform mixing of biomass particles with the bed material in fluidized bed reactors. In addition, if catalyst is used as a bed material, it is very important to have uniform mixing of biomass with the catalyst particles throughout the pyrolysis process. If there is segregation between the biomass and the catalyst particles in the bed, there will be improper catalytic cracking of volatiles such as tar compounds.

Hence, to achieve improved conditions of heat and mass transfer during biomass pyrolysis, we need to focus on various parameters such as the effects of superficial gas velocity, biomass particle density and size, which can potentially affect the mixing /segregation behavior in a fluidized bed reactor. Therefore, a multi-fluid model has been proposed for examining the fluidization of biomass particles with other solid phases such as biochar particles in the reactor.

MODEL DESCRIPTION

A cold flow model for bubbling fluidized bed reactor was developed using the Eulerian approach which considered the primary gas phase as well as two secondary solid phases, for the bed medium and the biomass particles

respectively. To simulate the hydrodynamic behavior of the dispersed phases of biomass and biochar particles, mass and momentum transfer with fluctuating kinetic energy of particles were considered. For the gas phase, the momentum transport was defined using the Navier- Stokes equations. For the solid phases, in addition to the Navier-Stokes equations, a set of constitutive relations for several transport properties such as the granular temperature, pressure and viscosity were also included.

Conservation Equations

The general conservation equations were derived for mass, momentum and kinetic energy of solid phases by incorporating the concept of phasic volume fraction (the volume fraction representing the space occupied by each phase). Some additional closure laws such as for gas-solid and solid-solid drag coefficients, solid shear and bulk viscosity, and collision parameters were also implemented (ANSYS FLUENT Guide, 2010).

Conservation of mass

The average mass balance of each phase was calculated using the continuity equation:

$$\frac{\partial\left(\alpha_q \rho_q\right)}{\partial t} + \nabla.\left(\alpha_q \rho_q \vec{v}_q\right) = 0 \qquad (1)$$

Conservation of momentum

For gas phase -

$$\frac{\partial\left(\alpha_g \rho_g \vec{v}_g\right)}{\partial t} + \nabla.\left(\alpha_g \rho_g \vec{v}_g \vec{v}_g\right) = -\alpha_g \nabla p + \nabla.\bar{\tau}_g + \alpha_g \rho_g \vec{g} + \sum_{s=1}^{n} \vec{R}_{gs} \qquad (2)$$

For solid phase (s =1, 2, …, n) -

$$\frac{\partial\left(\alpha_s \rho_s \vec{v}_s\right)}{\partial t} + \nabla.\left(\alpha_s \rho_s \vec{v}_s \vec{v}_s\right) = -\alpha_s \nabla p - \nabla p_s + \nabla.\bar{\tau}_s + \alpha_s \rho_s \vec{g} + \sum_{l=1}^{N} \vec{R}_{ls} \qquad (3)$$

here, R defines the interaction force between different phase in terms of momentum exchange/drag coefficient.

Conservation of Fluctuating Kinetic Energy (for solid phases)

The kinetic energy of fluctuating particle motion has been represented using the granular temperature of solid phase (θ_s), which is proportional to mean square of fluctuating velocity of solid particles.

$$\frac{3}{2}\left[\frac{\partial\left(\alpha_s \rho_s \theta_s\right)}{\partial t} + \nabla.\left(\alpha_s \rho_s \vec{v}_s \theta_s\right)\right] = -\left(p_s \bar{I} + \bar{\tau}_s\right):\nabla \vec{v}_s + \nabla.\left(k_{\theta_s} \nabla \theta_s\right) - \gamma_{\theta_s} + \Phi_{ls} \qquad (4)$$

Constitutive Relations

Similar to thermal motion of gas molecules, the intensity of random motion of particles arising from particle-particle collisions determines the stresses, viscosity and pressure of the solid phase. These relations are given in Appendix A.

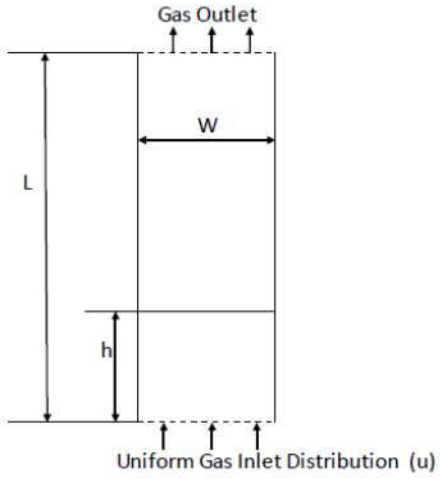

Figure 1: Schematic diagram of geometry

CFD Simulation Scheme

The coupled equations of phasic momentum, shared pressure and phasic volume fraction for a given multi-phase flow have been solved using ANSYS FLUENT version 13.0. The Phase Coupled SIMPLE algorithm has been utilized for solving these equations. In this scheme, the coupled individual phase velocities are solved in a segregated manner. With this, a pressure correction equation is formulated based on the total volume continuity. The coefficients for the pressure correction equation were also derived from the coupled momentum equations.

Solution Procedure, Initial and Boundary Conditions

All the simulations were carried out in a 2-dimensional fluidized bed reactor domain as shown in Figure 1. The simulation domain was divided into a fixed number of control volumes by defining grid cells in both horizontal and vertical directions. The equations were solved using the upwind differencing scheme for spatial discretization, and implicit scheme for transient formulation with a time step size of 10^{-4} seconds. An initial bed height of given volume fractions of biomass and fluidizing bed material was specified at the start of each simulation. The simulations were conducted for a period of 30 seconds of real time. The time-averaged parametric values were taken from 10 to 30 seconds of simulation results.

For the gas phase, the initial velocity was specified at the bottom of the bed. For the granular phases, the velocities have been considered as zero at the start of any simulation. A pressure boundary conditions was used at the top of the bed, which was fixed to a reference value of 1 atm.

For the gas phase, a no-slip boundary condition was considered on the walls. For the granular phases, the shear force at the walls was defined according to the relationship given by Sinclair and Jackson (1989).

RESULTS AND DISCUSSION

Since currently there are no experimental data available for "biomass-biochar" systems, initial simulations were carried out with biomass (rice husk) and "sand" , and the results were compared with exiting literature data (Qiaoqun et al., 2005). After the model was validated, simulations were conducted for the mixtures of biomass and biochar particles. In this study, a pine char was used as the bed material for analyzing fluidization of the pinewood or rice husk as the biomass. The pine char of 1 mm (Geldart B) diameter was used for the simulation. The averaged mass fraction of pinewood or rice husk was kept at 5.82 wt% in the biomass-biochar mixture. The biomass, sand and biochar particles were considered mono-sized and spherical in shape for the present modelling purposes. The conditions employed in the simulation are summarized in Table 1.

Table 1: Modelling conditions

Reactor height, L	2000 mm
Reactor diameter, W	450 mm
Grid cells in vertical direction	160
Grid cells in horizontal direction	75
Initial bed height, h	380 mm
$Diameter_{pinewood}$	1.54 and 2.5 mm
$Diameter_{sand}$	440 µm
$Diameter_{biochar}$	1 mm
$Density_{pinewood}$	584 kg/m^3
$Density_{rice\ husk}$	950.6 kg/m^3
$Density_{sand}$	2600 kg/m^3
$Density_{biochar}$	1470 kg/m^3
Coefficient of $restitution_{pinewood}$	0.6
Coefficient of $restitution_{biochar}$	0.9
Initial volume $fraction_{pinewood}$	0.081
Initial volume $fraction_{biochar/sand}$	0.519

Figure 2 suggests that the time averaged rice husk mass distribution at a superficial gas velocity of 0.79 m/s was in agreement between the simulation results and the experimental data (Qiaoqun et al, 2005) along the dimensionless bed height. Some discrepancy between the simulation and experimental results occurred in the top section of the bed because of possible experimental error, which becomes apparent on calculating the weighted average of rice husk mass fraction by considering the area under the experimental data points in Figure 2. The calculated value of average rice husk from experimental data was approximately 6.3% compared to actual initial value of 5.82%.

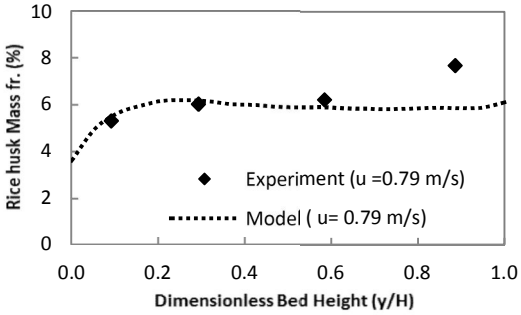

Figure 2: Time averaged rice husk mass distribution comparison with experimental results

The calculation of the minimum fluidization velocity (u_{mf}) of the biomass-biochar mixture was performed using the relationship of Chitester et al. (1984). Due to very small amount of biomass as compared to biochar in the mixture, the u_{mf} of the biomass-biochar mixture was found to be around 0.45 m/s for both pinewood and rice husk of 1.54 mm average diameter. However, the u_{mf} of pinewood of 2.5 mm is around 0.46 m/s, slightly higher than 1.54 mm size.

Figure 3 qualitatively shows the fluidization behavior of pinewood particles in the biochar bed, which was initially patched to have a uniform volume fraction of both solid phases. It can be seen from Figure 3(a), the bubbles only started to form at the minimum fluidization velocity. On increasing the gas velocity to above minimum fluidization velocity (as shown in Figure 3(b) and 3(c)), there was an increase in the average bubble size which led to increase in the movement of the pinewood particles along the bed height. This vigorous movement of particles with bubbles favours the mixing of the solid phases of different densities and sizes along the bed height.

The time averaged mass distribution of the pinewood particles with respect to the dimensionless bed height at different gas velocities is shown in Figure 4. The pinewood mass fraction is based on total solids only, without considering the gas phase. Since the pinewood particles are lighter, they behaved as flotsam, while the heavier biochar particles behaved as jetsam in the bed. The simulation results suggested that there was uniform segregation between the rice husk and char particles across the bed height at the minimum fluidization velocity. On increasing the velocity just above u_{mf} (at u = 0.54 m/s), the bubble movement from the bottom to the top of the bed leads to distribution of the pinewood particles along the bed height. But there was some segregation between the two phases as the mixing due to the formation of small bubbles was weak at this velocity. The mixing between the two solid phases became uniform at velocities close to 2.5 times of the minimum fluidization velocity (at u = 1.14 m/s).

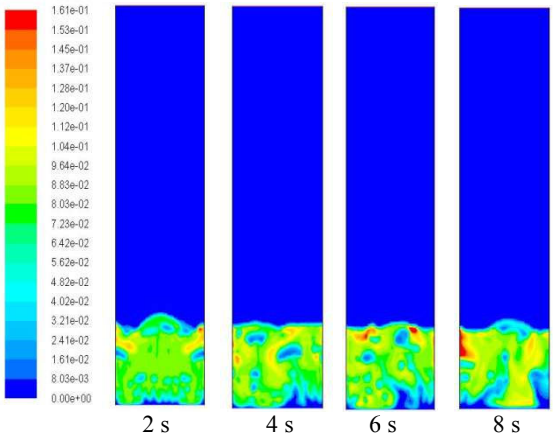

3(a). u = 0.45 m/s (u/u_{mf} = 1)

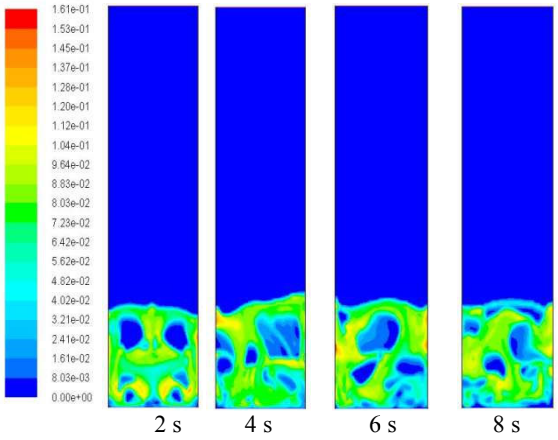

3(b). u = 0.68 m/s (u/u_{mf} = 1.5)

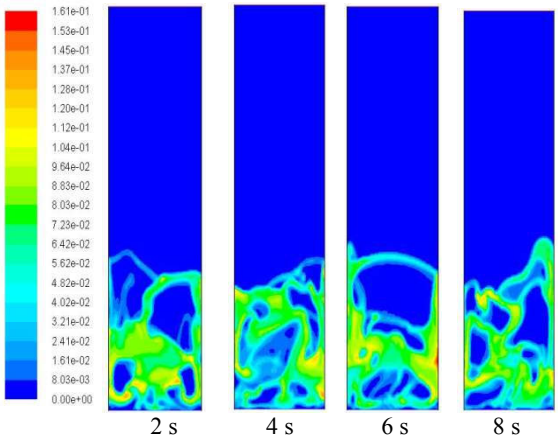

3(c). u = 1.14 m/s (u/u_{mf} = 2.5)

Figure 3: Volume fraction profile of pinewood. (5.82 wt%) for different superficial gas velocities

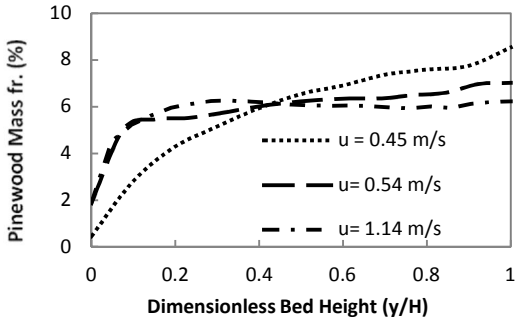

Figure 4: Time averaged pinewood mass distribution at different gas velocities

It is clear from Figure 5 that for a fixed superficial gas velocity, on changing the density of biomass particles in the bed, there was considerable change in the biomass distribution across the bed height. For example, for gas superficial velocity of 0.68 m/s, on increasing the biomass density from 584 kg/m^3 (pinewood) to 950.6 kg/m^3 (rice husk) (the average particle diameter is same for both types of biomass), the segregation of biomass particles in the biochar bed decreased. This leads to better distribution of rice husk particles in the bed compared to to pinewood particles which had significantly lower concentration in the bottom part of the bed and higher in top section of the bed due to segregation. This was mainly because of the density difference between rice husk and biochar particles are less as compared to the difference between pinewood and biochar particles in the bed.

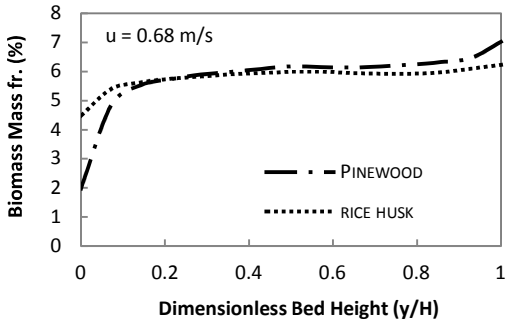

Figure 5: Time averaged mass distribution of pinewood and rice husk

Figure 6 shows the pinewood mass distribution for two different particle sizes with respect to dimensionless bed height. According to results, there was not considerable difference in the distribution of biomass particles in the biochar bed for average pinewood particle diameter of 1.54 and 2.5 mm. As the mass fraction of biomass was less than the biochar in the bed, the effect of change of biomass particle diameter was negligible on mixing/segregation behavior of both solid phases.

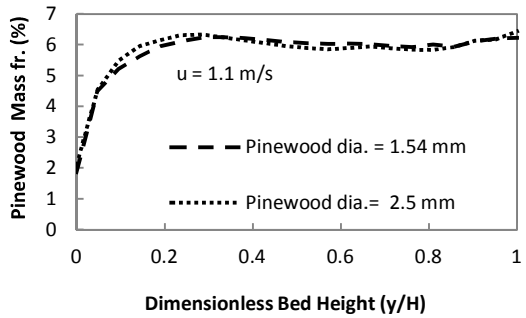

Figure 6: Time averaged pinewood mass distribution for different particle sizes in the biochar bed

The time-averaged distribution of vertical velocities of pinewood (5.82 wt%) and biochar particles at superficial gas velocity of 0.54 m/s are shown in Figure 7. It is clear that in the centre of the bed, both pinewood and biochar particles flow upward with positive velocities, while near the walls, they flow downward with negative velocities. The velocity of pinewood particles was marginally higher than biochar particles in centre region of the bed. However, there is not much difference in their velocities in the wall region.

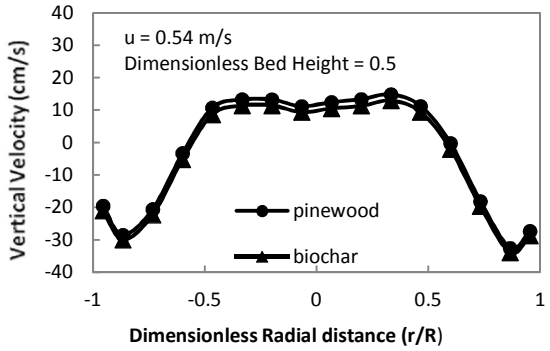

Figure 7: Distribution of vertical velocity of pinewood and biochar particles.

CONCLUSIONS

A multi-phase hydrodynamic model for studying the behavior of biomass in poly-dispersed systems has been developed. Simulations were performed to study the effect of superficial gas velocity on fluidization characteristics of the pinewood-biochar mixture. It was found that increasing the gas superficial velocities to above the minimum fluidization velocity of the mixture led to an enhanced mixing of the solid phases with bubbles in the bed. It was also found that, in addition to the superficial gas velocity, the biomass particle density had a significant impact on the mixing/segregation patterns of the biomass, whilst the biomass particle diameter had only a little impact.

REFERENCES

ABDULLAH, M. Z., HUSAIN, Z., YIN PONG, S.L., (2003), "Analysis of cold flow fluidization test results for various biomass fuels", *Biomass and Bioenergy,* **24**(6), 487-494.

ANSYS FLUENT Theory Guide, version 13.0, (2010).

CHITESTER, D. C., KORNOSKY, R. M., FAN, L.S., DANKO, J.P., (1984),"Characteristics of fluidization at high pressure." *Chemical Engineering Science,* **39**(2), 253-261.

CLARKE, K. L., PUGSLEY, T., HILL, G.A., (2005), "Fluidization of moist sawdust in binary particle systems in a gas–solid fluidized bed", *Chemical Engineering Science***, 60**(24), 6909-6918.

CUI, H. and GRACE, J. R., (2007), "Fluidization of biomass particles: A review of experimental multiphase flow aspects", *Chemical Engineering Science*, **62**(1-2), 45-55.

DEMIRBAS, A. and ARIN, G., (2002), "An Overview of Biomass Pyrolysis" *Energy Sources,* **24**(5), 471-482.

DEMIRBAS, M.F., BALAT M., BALAT H., (2009) "Potential contribution of biomass to the sustainable energy development", *Energy Conversion and Management*, **50**(7), 1746-1760.

QIAOQUN, S., HUILIN, L., WENTIE, L., YURONG, H., LIDAN, Y., GIDASPOW, D. (2005), "Simulation and experiment of segregating/mixing of rice husk-sand mixture in a bubbling fluidized bed", *Fuel,* **84**(14-15), 1739-1748.

RAO, R.T. and BHEEMARASETTI, J. V. R., (2001), "Minimum fluidization velocities of mixtures of biomass and sands", *Energy,* **26**(6), 633-644.

SINCLAIR, J. L. and JACKSON, R., (1989), "Gas-particle flow in a vertical pipe with particle-particle interactions", *AIChE Journal*, **35**(9), 1473-1486.

ZHANG, Y., JIN, B., ZHONG, W., (2009), "Experimental investigation on mixing and segregation behavior of biomass particle in fluidized bed", *Chemical Engineering and Processing: Process Intensification*, **48**(3), 745-754.

ZHONG, W., JIN, B., ZHANG, Y., WANG, X., XIAO, R., (2008), "Fluidization of Biomass Particles in a Gas−Solid Fluidized Bed", *Energy & Fuels* **22**(6), 4170-4176.

APPENDIX A

(1) Gas phase stress-strain tensor

$$\bar{\tau}_g = \alpha_g \mu_g \left[\nabla \vec{v}_g + \nabla \vec{v}_g{}^T \right] - \frac{2}{3} \alpha_g \mu_g \nabla . \vec{v}_g \bar{I}$$

where, μ_g = Gas-phase viscosity

(2) Solid phase stress-strain tensor

$$\bar{\tau}_s = \alpha_s \mu_s \left[\nabla \vec{v}_s + \nabla \vec{v}_s{}^T \right] + \alpha_s (\lambda_s - \frac{2}{3} \mu_s) \nabla . \vec{v}_s \bar{I}$$

where μ_s = Shear viscosity of s^{th} solid phase

and λ_s = Bulk viscosity of s^{th} solid phase

(3) Solids Pressure

The solid pressure consists a kinetic term (the first term) and other terms due to particle collisions.

$$p_s = \alpha_s \rho_s \theta_s + 2\rho_s (1 + e_{ss}) \alpha_s{}^2 g_{0,ss} \theta_s$$

where e_{ss} = coefficient of restitution for particle collisions and $g_{0,ss}$ = radial distribution function.

For a multi- phase system (N number of phases), this equation has been written by considering the presence of other phases as well.

$$p_l = \alpha_l \rho_l \theta_l + \sum_{l=1}^{N} 2 \frac{d_{ls}^3}{d_l^3} (1 + e_{ls}) g_{0,ls} \alpha_l \alpha_s \rho_l \theta_l$$

where $d_{ls} = (d_l + d_s)/2$, is the average diameter and $e_{ls} = (e_l + e_s)/2$.

(4) Radial distribution function

This is a correction factor that alters the probability of collisions between grains in dense solid granular phase. Its value varies from 1 for dilute solid phase to infinity for compact solid phase.

For N solid phases, the function has been defined as:

$$g_{0,ll} = \frac{1}{(1 - \frac{\alpha_s}{\alpha_{s,max}})} + \frac{3}{2} d_l \sum_{k=1}^{N} \frac{\alpha_k}{d_k}$$

where $\alpha_s = \sum_{k=1}^{N} \alpha_k$ (k are solid phases only) and

$\alpha_{s,max} = \sum_{k=1}^{N} \alpha_{k,max}$ ($\alpha_{k,max}$ = Maximum packing limit of k^{th} solid = 0.63),

whereas the equation at contact for mixtures (l^{st} and s^{th} solid phase) has been considered as:

$$g_{0,ls} = \frac{d_m g_{0,ll} + d_l g_{0,ss}}{d_s + d_l}$$

(5) Solid phase shear viscosity

This is made up of kinetic, collisional and frictional viscosity of the solid phase.

$$\mu_s = \mu_{s,kin} + \mu_{s,col} + \mu_{s,fr}$$

where $\mu_{s,kin} = \frac{\alpha_s d_s \rho_s \sqrt{\theta_s \pi}}{6(3 - e_{ss})} [1 + \frac{2}{5} (1 + e_{ss})(3e_{ss} - 1) \alpha_s g_{0,ss}]$,

and $\mu_{s,col} = \frac{4}{5} \alpha_s d_s \rho_s g_{0,ss} \sqrt{\theta_s / \pi} (1 + e_{ss}) \alpha_s$

For dense flow systems, where secondary volume fraction for solid phase is close to the packing limit (considered to be around 0.61), the generation of stress is majorly because of friction between particles and the instantaneous collision between particles are less important. In such case, frictional viscosity has to be included in solid phase shear viscosity expression.

$$\mu_{s,fr} = \frac{p_s \sin\phi}{2\sqrt{I_{2D}}}$$

where p_s = solid phase pressure

ϕ = angle of internal friction= 30^0

I_{2D} = second invariant of deviatoric stress tensor, and

$P_{friction} = Fr \frac{(\alpha_s - \alpha_{s,min})^n}{(\alpha_{s,max} - \alpha_s)^p}$ and

Fr = $0.1\alpha_s$, n= 2 and p =5 (9)

(6) Solid phase bulk viscosity

The resistance of the granular particles due to compression and expansion is described as:

$$\lambda_s = \frac{4}{5} \alpha_s d_s \rho_s g_{0,ss} \sqrt{\theta_s / \pi} (1 + e_{ss}) \alpha_s$$

(7) Drag coefficient between fluid (gas) and solid phase -

When α_g > 0.8, the fluid-solid momentum exchange coefficient is of the form:

$$K_{gs} = \frac{3}{4} C_D \frac{\alpha_s \alpha_g \rho_g |\vec{v}_s - \vec{v}_g|}{d_s} \alpha_g^{-2.65} \quad (10)$$

where, $C_D = \frac{24}{\alpha_g Re_s} [1 + 0.15(\alpha_g Re_s)^{0.687}]$

Reynolds Number, $Re_s = \frac{\rho_g d_s |\vec{v}_s - \vec{v}_g|}{\mu_g}$

and, when α_g < 0.8,

$$K_{gs} = 150 \frac{\alpha_s (1 - \alpha_g) \mu_g}{\alpha_g d_s^2} + 1.75 \frac{\rho_g \alpha_s |\vec{v}_s - \vec{v}_g|}{d_s}$$

(8) Drag coefficient between solid and solid phase

$$K_{ls} = \frac{3(1 + e_{ls})\left(\frac{\pi}{2} + C_{fr,ls}\frac{\pi^2}{8}\right) \alpha_s \rho_s \alpha_l \rho_l (d_l + d_s)^2 g_{0,ls}}{2\pi(\rho_l d_l^3 + \rho_s d_s^3)} |\vec{v}_l - \vec{v}_s|$$

where $C_{fr,ls}$ = coefficient of friction between l^{st} and s^{th} solid phase-particles = 0

(9) Diffusion coefficient of granular energy

This coefficient contributes to the diffusive component of granular energy.

$$k_{\theta_s} = \frac{15 d_s \rho_s \alpha_s \sqrt{\theta_s \pi}}{4(41 - 3\eta)} [1 + \frac{12}{5} \eta^2 (4\eta - 3) \alpha_s g_{0,ss} + \frac{16}{15\pi} (41 - 33\eta) \eta \alpha_s g_{0,ss}] \quad \text{where } \eta = (1 + e_{ss})/2$$

(10) Collisional dissipation of energy

The energy dissipation rate within s^{th} solid phase due to collision between particles, is represented as

$$\Gamma_{\theta_s} = \frac{12(1 - e_{ss}^2) g_{0,ss}}{d_s \sqrt{\pi}} \rho_s \alpha_s^2 \theta_s^{3/2}$$